Direct Photon Production in Au + Au Collisions at $\sqrt{s_{NN}}$ == 200 GeV at STAR

Chi Yang[*][†]

Shandong University, China
E-mail: chiyang@sdu.edu.cn

Photons are unique probes to study the fundamental properties of the hot and dense medium created in ultra-relativistic heavy-ion collisions. By minimal interactions with the medium, the photons can bring information about the dynamics of the entire time evolution of the medium. We report the direct photon invariant yields in the transverse momentum ranges $1 < p_T < 3$ GeV/c and $5 < p_T < 10$ GeV/c at mid-rapidity derived from the low-mass e^+e^- invariant mass continuum in 0-80% minimum-bias Au+Au collisions at $\sqrt{s_{NN}} = 200$ GeV. Centrality dependence of direct photon yields is presented. A clear excess of the invariant yield relative to the yield in $p + p$ scaled by nuclear overlap function T_{AA} is observed in the p_T range $1 < p_T < 3$ GeV/c. The production follows T_{AA} scaling at $p_T > 6$ GeV/c.

---

[*]Speaker.

[†]for the STAR Collaboration

1. Introduction

Direct photon production is a unique probe in the study of the fundamental properties of the hot and dense medium created in ultra-relativistic heavy-ion collisions. It stands for all the produced photons except those from hadron decays in the last stage of the collisions. Due to the minimal interactions with the medium, the photons can bring information about the dynamics from the whole time evolution of the medium [1]. Measurements at the RHIC [2, 3] and the LHC [4, 5] have shown that the production of the high p_T direct photons in heavy-ion collisions is consistent with the $p + p$ result scaled by the nuclear overlap function T_{AA} for $p_T > 5$ GeV/c, which indicates that the dominant contribution is from hard processes in high p_T.

At $1 < p_T < 3$ GeV/c, thermal contributions from the hadronic medium and Quark-Gluon Plasma (QGP) play a major role [6]. At $3 < p_T < 5$ GeV/c, the interaction of high energy partons with the QGP (e.g. $q + g \rightarrow \gamma + q$) has been predicted to contribute a major part of the direct photon production [6]. An excess of direct photon yields compared with the T_{AA} scaled $p + p$ production was found in central Au+Au at $\sqrt{s_{NN}} = 200$ GeV in the p_T range $0.4 < p_T < 4.0$ GeV/c [7, 8] and in central Pb+Pb at $\sqrt{s_{NN}} = 2.76$ TeV for $0.9 < p_T < 2.1$ GeV/c [5]. The excess increases exponentially as p_T decreases.

There are two methods to measure the direct photons created from high energy heavy ion collisions. One is to measure all the inclusive photons and then subtract the photons from hadron decays, just like the definition of direct photon. The other one, used in this article, is the virtual photon method in which one measures virtual photons via their associated e^+e^- pairs and then deduces the direct photon from the relationship between virtual photon and direct photon yields [7]. In this article, we report the direct photon invariant yields in the transverse momentum ranges $1 < p_T < 3$ GeV/c and $5 < p_T < 10$ GeV/c at mid-rapidity derived from the low-mass e^+e^- invariant mass continuum in 0-80% minimum-bias Au+Au collisions at $\sqrt{s_{NN}} = 200$ GeV. Comparisons to model calculations with thermal contributions from the hadronic medium and QGP are discussed.

2. Experiment and Data Analysis

The data used in this analysis are from Au+Au collisions at $\sqrt{s_{NN}} = 200$ GeV collected by the STAR detector in year 2010 (run 10) and 2011 (run 11). There are 258 million and 488 million minimum-bias (0-80%) events from run 10 and run 11, respectively, passing data quality assurance and vertex selection. In addition, 220 million 0-10% centrality triggered events from run 10 are used.

The main subsystems used for electron identification are the Time Projection Chamber (TPC) [9] and the Time-Of-Flight detector (TOF) [10] for the minimum-bias and central triggered events. The analysis details of e^+e^- measurements from minimum-bias and central triggered events are presented in Ref. [11]. For BEMC-triggered events, the electron(positron) identification(EID) for $p_T^e > 4.5$ GeV/c uses a combination of the TPC and BEMC information. The 39 million BEMC triggered events are equivalent to 6.5 billion minimum-bias events. This trigger setting enhanced the trigger capability for high p_T events significantly.

The e^+e^- invariant mass spectrum in this analysis is constructed within the STAR acceptance ($p_T^e > 0.2$ GeV/c, $|\eta^e| < 1$, $|y^{ee}| < 1$) and corrected on efficiency, where p_T^e is the electron p_T, η^e

is the electron pseudo-rapidity, and y^{ee} is the rapidity of electron-positron pairs. Fig. 1 shows the spectra in different p_T ranges. The results at $p_T < 3$ GeV/c are the combined results from run 10 and run 11 data. At $p_T > 5$ GeV/c, they are from the BEMC-triggered data. The limitation of the e^+e^- pair p_T range in these two data sets is due to a large hadron contamination for electrons at $p_T^e > 2$ GeV/c in minimum-bias and central triggered data and a low trigger efficiency for electrons at $p_T^e < 4.5$ GeV/c in the BEMC-triggered data.
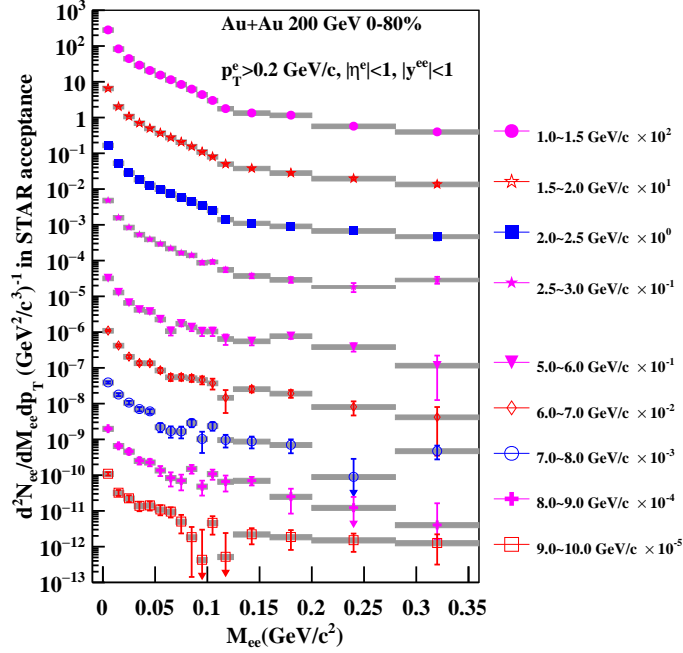
Figure 1: (Color online) e^+e^- invariant mass spectra in the low-mass range for 0-80% Au+Au collisions at $\sqrt{s_{NN}} = 200$ GeV [13]. The spectra in various p_T ranges as indicated in the figure are scaled by different factors for clarity. The error bars and the shaded bands represent the statistical and systematic uncertainties, respectively.

The detailed methodology about how to measure direct photon from low-mass e^+e^- continuum is presented in Ref. [12]. The direct photon yields are extracted by fitting the e^+e^- invariant mass spectra in the low mass region with two components. In the two-component fitting function $(1-r)f_{cocktail} + rf_{dir}$, $f_{cocktail}$ is the shape of the normalized hadronic cocktail mass distribution within the STAR acceptance, f_{dir} is the shape of the normalized internal conversion mass distribution from direct photons within the STAR acceptance, and r is the only fitting parameter. We normalized both $f_{cocktail}$ and f_{dir} to data points for $M_{ee} < 0.03$ GeV/c^2, separately. In this mass region the shapes of $f_{cocktail}$ and f_{dir} are identical, thus the fitting function in this mass region is independent of r. The parameter r can be interpreted as the ratio of direct photon to inclusive photon yields. The range for the two-component fit to data is $0.10 < M_{ee} < 0.28$ GeV/c^2. Figure 2 shows an example of the two-component fit for $2.0 < p_T < 2.5$ GeV/c. The uncertainties in the e^+e^- mass spectrum are the quadrature sum of statistical and point-to-point systematic uncertainties. With the r value derived for each p_T bin, one can obtain the direct virtual photon invariant yield. All details of this analysis can be found in Ref. [13].

2
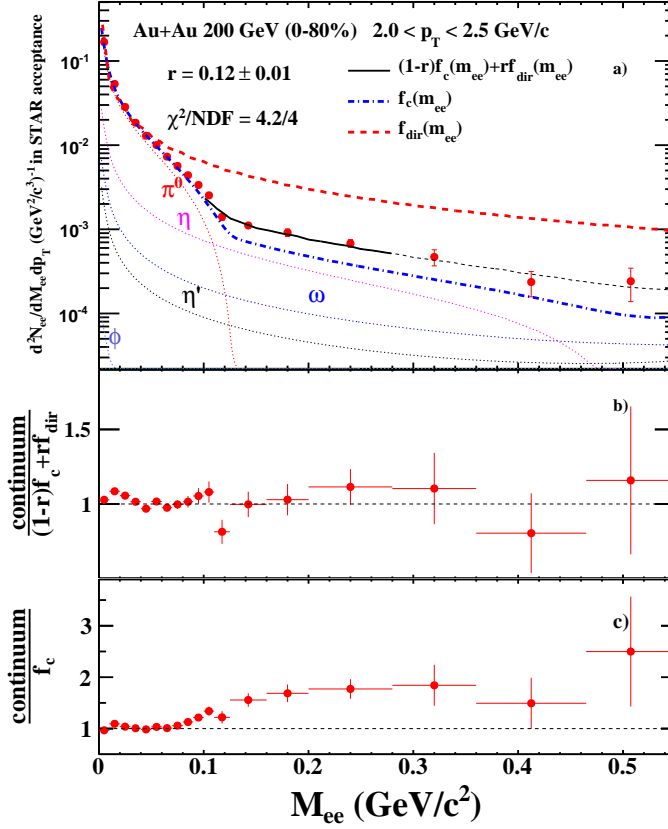
Figure 2: (Color online) Panel (a): The two-component fitting function results for the Au+Au e^+e^- spectra at $2.0 < p_T < 2.5$ GeV/c. The dot-dashed and dashed lines represent the normalized cocktail and internal conversion from direct photons, respectively. The solid line is the fit to the data in the range $0.10 < M_{ee} < 0.28$ GeV/c^2. The light dashed-line is the extrapolation of the fit function outside the fit range. The dotted lines represent different cocktail components. Panel (b): The data divided by the fit model as a function of M_{ee}. Panel (c): The data divided by the cocktail component as a function of M_{ee} [13].

3. Result

Figure 3 shows the fraction of direct photon over inclusive photon yields compared with the ratio of T_{AA} scaled Next-to-Leading-Order (NLO) perturbative QCD (pQCD) predictions to inclusive photon yields as function of p_T. The curves represent $T_{AA} \frac{d^2\sigma_\gamma^{NLO}(p_T)}{2\pi p_T dp_T dy} / \frac{d^2N_\gamma^{inc}(p_T)}{2\pi p_T dp_T dy}$ showing the scale dependence of the theory [14] in which T_{AA} is the nuclear overlap factor, $\frac{d^2\sigma_\gamma^{NLO}(p_T)}{2\pi p_T dp_T dy}$ is the p_T-differential invariant cross section for direct photons obtained from Ref. [15], and $\frac{d^2N_\gamma^{inc}(p_T)}{2\pi p_T dp_T dy}$ is the inclusive photon p_T-differential invariant yield. The data show consistency with NLO pQCD calculations within uncertainties at $p_T > 6$ GeV/c. Clear enhancement in data compared to the calculation is observed at $1 < p_T < 3$ GeV/c. The data point at $p_T = 5.5$ GeV/c is about 2.5σ higher than the calculation.

Figure 4 shows centrality dependence of the invariant yields of the direct photons in Au+Au collisions at $\sqrt{s_{NN}} = 200$ GeV. Due to large systematic uncertainties in 1-2 GeV/c in central col-
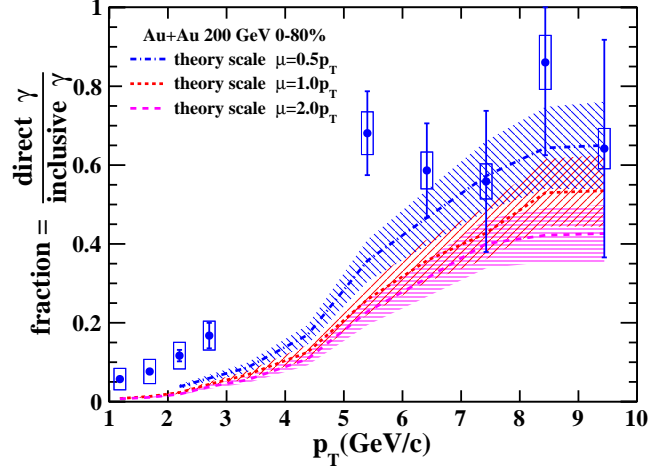
Figure 3: (Color online) The ratio of direct photon to inclusive photon yields compared with the ratio of T_{AA} scaled NLO pQCD predictions to inclusive photon yields for 0-80% Au+Au collisions at $\sqrt{s_{NN}} = 200$ GeV [13]. The three curves correspond to pQCD calculations with different renormalization (μ_R) and factorization scales (μ_F), assuming $\mu_R = \mu_F = \mu$. The error bars and the boxes represent the statistical and systematic uncertainties, respectively. The shaded bands on the curves represent the systematic uncertainties for inclusive photon measurements, which are about 15%.
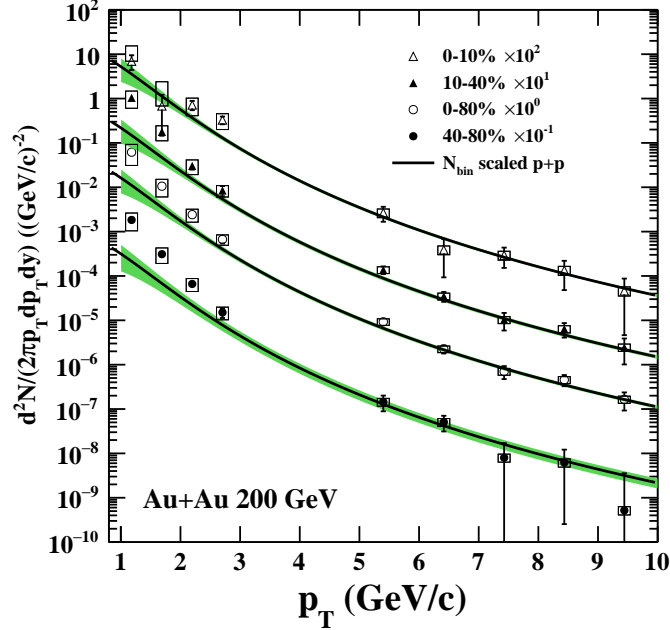
Figure 4: (Color online) Centrality dependence of the direct photon invariant yields as a function of p_T in Au+Au collisions at $\sqrt{s_{NN}} = 200$ GeV [13]. The solid curves represent a power-law fit to PHENIX 200 GeV $p + p$ results [8, 15], scaled by T_{AA}. The bands on the curves represent the uncertainties in the parameterization and in T_{AA}. The error bars and boxes represent the statistical and systematic uncertainties, respectively.
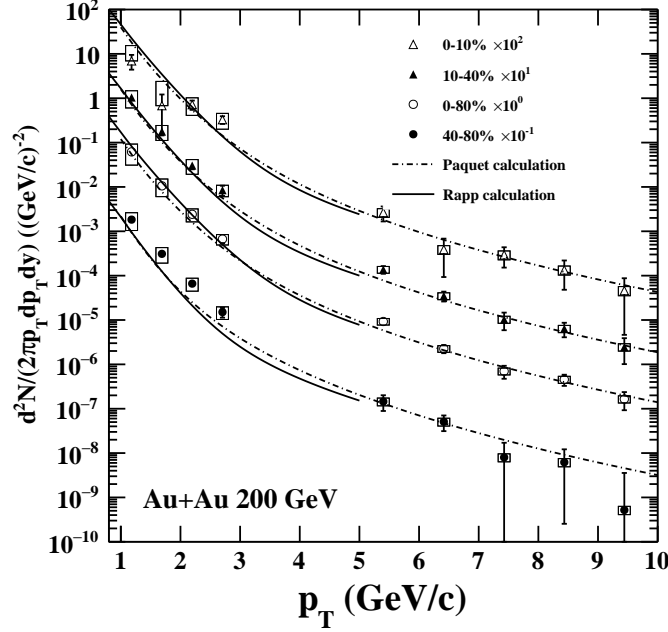
Figure 5: The direct photon invariant yields as a function of p_T in Au+Au collisions at $\sqrt{s_{NN}} = 200$ GeV compared to model predictions [13] from Rapp et al. [16, 17] and Paquet et al. [18]. The statistical and systematic uncertainties are shown by the bars and boxes, respectively.

lisions, we only plot the upper half of the uncertainty boxes while the uncertainties are all symmetric. The $p + p$ result is parameterized by a power-law function [15]. The parameterized distribution is then scaled by T_{AA}, and compared to the Au+Au results in different centralities, as shown in the solid curves. The T_{AA} values calculated from a Glauber model for 0-10%, 10-40%, 0-80% and 40-80% Au+Au collisions at $\sqrt{s_{NN}} = 200$ GeV are $(941 \pm 26)/42mb$, $(391 \pm 30)/42mb$, $(292 \pm 20)/42mb$, and $(57 \pm 14)/42mb$, respectively. For $1 < p_T < 3$ GeV/c, the Au+Au results are higher than the T_{AA} scaled $p + p$ results, while at $p_T > 6$ GeV/c the Au+Au yield is consistent with the scaled $p + p$ expectation. We note that for $1 < p_T < 2$ GeV/c, the data points in 0-10% Au+Au collisions have larger uncertainties and are also consistent with the scaled $p + p$ expectations.

A comparison between STAR Au+Au data and model calculations from Rapp *et al*. [16, 17] and Paquet *et al*. [18] is shown in Fig. 5. For the direct photon production both models include the contributions from QGP thermal radiation, in-medium ρ meson and other mesonic interactions in the hadronic gas, and primordial contributions from the initial hard parton scattering. In Rapp's model, an elliptic thermal fireball evolution is employed for the bulk medium. The sum of the thermal medium and primordial contributions for the former case is shown in Fig. 5. In Paquet's model, a (2+1)-D hydrodynamic evolution is employed for the bulk medium. The comparison between the model and data shows that in the p_T range 1-3 GeV/c the dominant source is the thermal radiation, while the initial hard-parton scattering becomes dominant in p_T range 5-6 GeV/c. The comparison shows agreement between both model calculations and our measurement within uncertainties for all the other centralities except 40-80% centrality which includes most peripheral

collisions, where hydrodynamic calculations might not be applicable.

4. Summary

We measured the e^+e^- spectra and inferred direct photon production in Au+Au collisions at STAR at $\sqrt{s_{NN}} = 200$ GeV. The direct photon measurement based on the virtual photon method is extended to p_T of 5-10 GeV/c. In the p_T range 1-3 GeV/c, the direct photon invariant yield shows a clear excess in 10-40% and 40-80% central Au+Au over the T_{AA} scaled $p + p$ results. In the p_T range above 6 GeV/c, there is no clear enhancement observed for all the centralities. The model predictions that include the contributions from the thermal radiation and initial hard-processes are consistent with our direct photon yield within uncertainties in central and mid-central collisions. In 40-80% centrality, the model calculations are systematically lower than our data for $1 < p_T < 3$ GeV/c.

References

[1] G. David, R. Rapp and Z. Xu, Phys. Rept. **462**, 176 (2008).

[2] M. Harrison, T. Ludlam, and S. Ozaki, Nucl. Instr. Meth. A **499**, 235 (2003).

[3] S. Afanasiev *et al.* [PHENIX Collaboration], Phys. Rev. Lett. **109**, 152302 (2012).

[4] S. Chatrchyan *et al.* [CMS Collaboration], Phys. Lett. B **710**, 256 (2012).

[5] J. Adam *et al.* [ALICE Collaboration], Phys. Lett. B **754**, 235 (2016).

[6] S. Turbide, C. Gale, E. Frodermann, and U. Heinz, Phys. Rev. C **77**, 024909 (2008).

[7] A. Adare *et al.* [PHENIX Collaboration], Phys. Rev. Lett. **104**, 132301 (2010).

[8] A. Adare *et al.* [PHENIX Collaboration], Phys. Rev. C **91**, 064904 (2015).

[9] M. Anderson *et al.*, Nucl. Instr. Meth. A **499**, 659 (2003).

[10] B. Bonner *et al.*, Nucl. Instr. Meth. A **508**, 181 (2003); M. Shao *et al.*, Nucl. Instr. Meth. A **492**, 344 (2002); J. Wu *et al.*, Nucl. Instr. Meth. A **538**, 243 (2005).

[11] L. Adamczyk *et al.* [STAR Collaboration], Phys. Rev. C **92**, 024912 (2015).

[12] A. Adare *et al.* [PHENIX Collaboration], Phys. Rev. C **81**, 034911 (2010).

[13] L. Adamczyk *et al.* [STAR Collaboration], arXiv:1607.01447.

[14] L.E. Gordon and W. Vogelsang, Phys. Rev. D **48**, 3136 (1993).

[15] S.S. Adler *et al.* [PHENIX Collaboration], Phys. Rev. Lett. **98**, 012002 (2007).

[16] H. van Hees, C. Gale, and R. Rapp, Phys. Rev. C **84**, 054906 (2011).

[17] H. van Hees, M. He, and R. Rapp, Nucl. Phys. A **933**, 256 (2015).

[18] J.-F. Paquet *et al.*, Phys. Rev. C **93**, 044906 (2016); J.-F. Paquet *et al.*, private communications.